Combustion Noise of Auxiliary Power Units

Christopher K.W. Tam* and Nikolai N. Pastouchenko†
Florida State Univeristy, Tallahassee, FL 32306-4510

Jeff Mendoza‡ and Dan Brown§
Honeywell Engine, Systems, and Services, Phoenix, AZ 85034

Noise from auxiliary power units (APU) is an important contributor to the overall level of ramp noise. Currently, ramp noise is regulated by international governing bodies as well as by individual airport. A significant component of APU noise is combustion noise. In this study, the unique spectral shape of APU combustion noise is identified. It is found that the spectral shape is the same regardless of engine size, power setting and directivity. Also, it is practically the same as that of open flame combustion noise. The frequency at the peak of the combustion noise spectrum is found to lie in the narrow range between 250 to 350 Hz. The peak sound pressure level of a given APU varies as the square of the fuel consumption rate. In the literature, suggestions have been made concerning a second combustion noise mechanism arising from the passage of hot entropy spots through the exhaust nozzle or constriction. In this investigation, no evidence has been found to indicate the existence of a second APU combustion noise component.

I. 1. Introduction

While noise from airplanes flying overhead is highly regulated, the noise generated by an aircraft while it is on the ground, typically parked at the ramp, is not regulated by large governing bodies like the FAA or JAA. Rather, the authorities of each airport set their own limitations and/or penalties for ramp noise levels based on a number of factors that may include the proximity of nearby housing or standards agreed upon with a labor union. The more stringent limitations are found at European airports, some of which require that all gas turbine auxiliary power units (APU), and consequently environmental control systems (ECS) be shut down 5 minutes after arrival at the gate and started no more than 5 minutes before the estimated time of departure. This requires the airline to hook into, and pay for, ground electric and conditioned air, something most would like to avoid. Many airports require that an airplane meet the International Civil Aviation Organization (ICAO), Annex 16, Attachment C recommended overall SPLs of 85 dBA at aircraft service locations and 90 dBA maximum along a 20-meter perimeter around the airplane. Some now require nighttime levels to be 5 dBA below the ICAO recommendations. Figure 1 and 2 show the ICAO noise recommendations with various service locations around an aircraft and sources of noise around a typical aircraft that contribute the overall ramp noise levels of the aircraft, respectively. Figure 3 is an isometric view of the aft end of an aircraft illustrating typical locations of an APU inlet and exhaust. The location of the inlet and exhaust interface with the airframe varies from installation to installation and can play a critical role in meeting customer noise requirements.

Airlines and the airframers, weigh a number of factors to determine the ramp noise level specifications for a new airplane. These include feedback from the airlines who will be purchasing the plane, the marketing strategy of the airframer, and what they feel is technically feasible. The ramp noise requirements for most commercial transport airplanes are equal to or below the ICAO recommended levels. For smaller planes in the business and small regional classes where APU installations are compact and distances are small between noise sources and receivers, often the specifications are more lenient.

Measured installed and component noise spectra indicate that APU exhaust noise dominates overall levels at many critical locations around most airplanes. Figure 4 contains measured overall sound pressure levels around two

* Robert O. Lawton Distinguished Professor, Department of Mathematics, Fellow AIAA.
† Postdoctoral Research Associate, Department of Mathematics.
‡ Engineer, Installation Aero and Acoustics, Senior Member AIAA..
§ Engineer, Installation Aero and Acoustics.

airplanes showing the distinct shape of APU exhaust noise directivity (lobes 60° from the centerline), and the extent to which exhaust noise drives levels around each airplane. A principal contributor to APU noise is combustion noise. This is the subject of the present study.

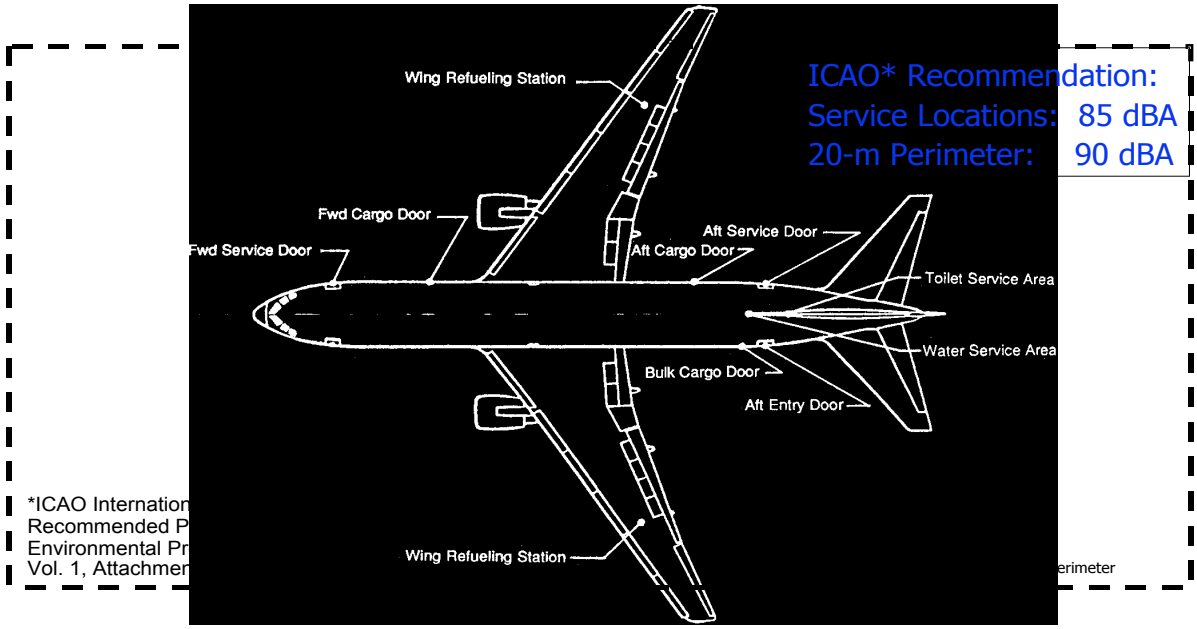

Figure 1. Service locations and ICAO Ramp Noise recommendations.

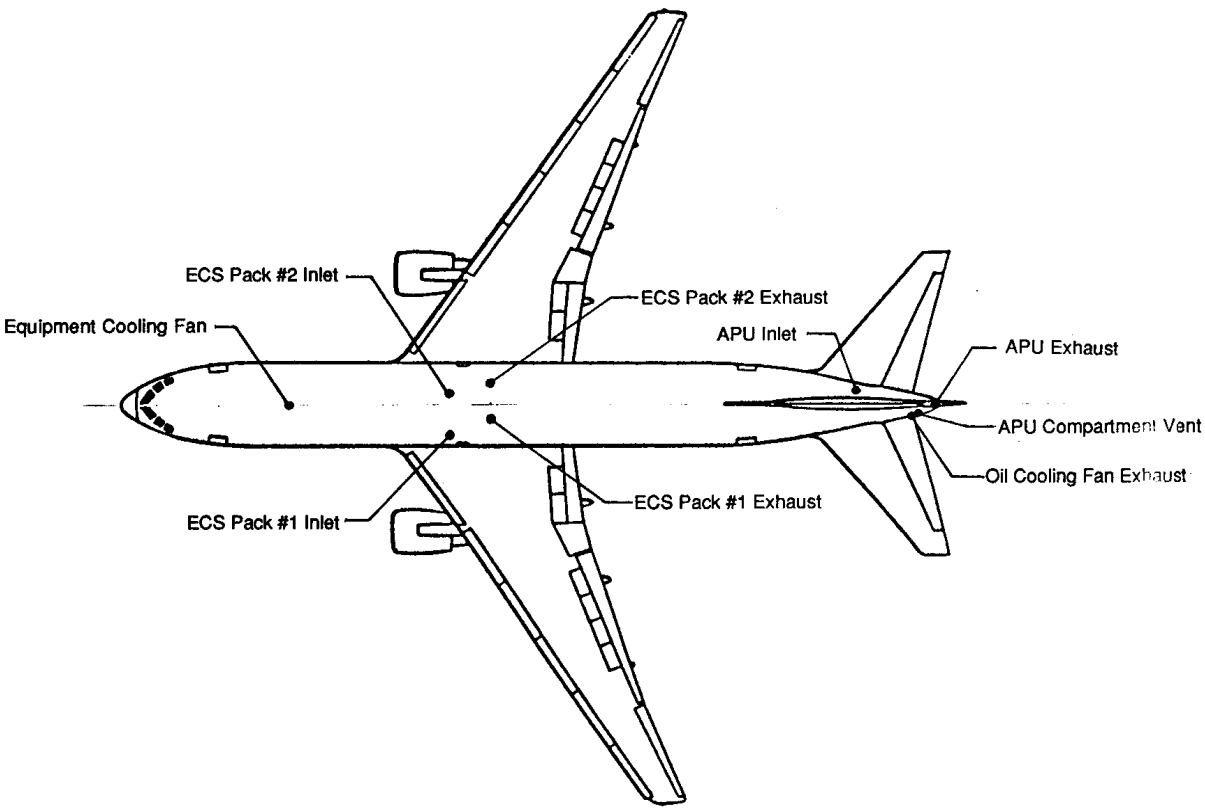

Figure 2. Sources of ramp noise.

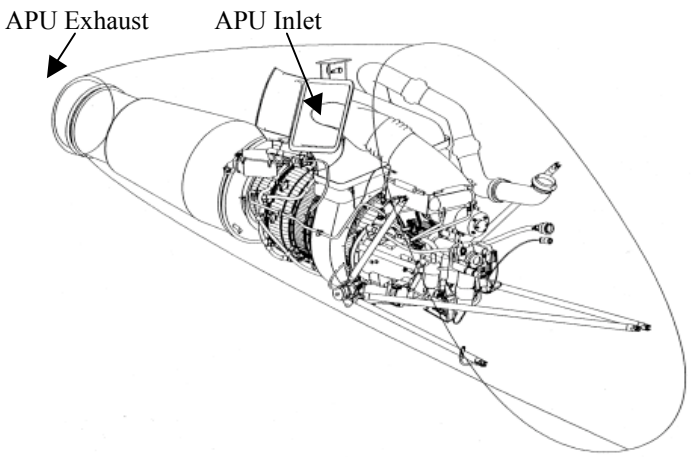

Figure 3. Isometric view of aircraft aft-end illustrating typical APU exhaust linlet and exhaust installation.

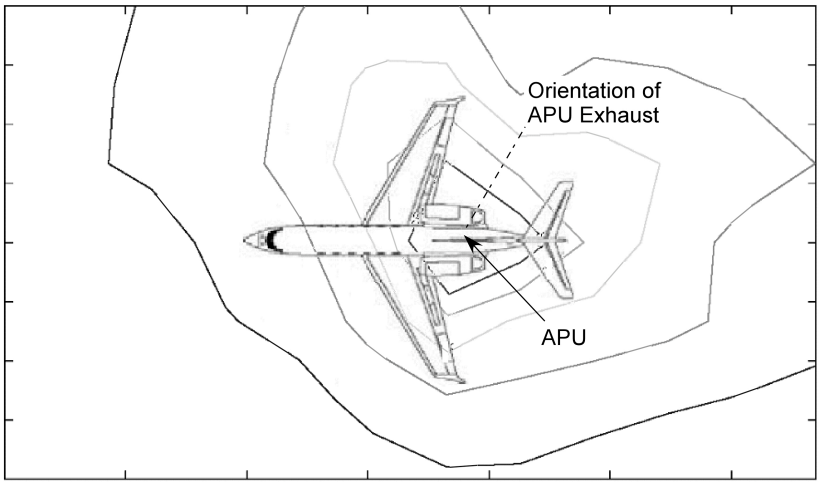

(a) Business aircraft

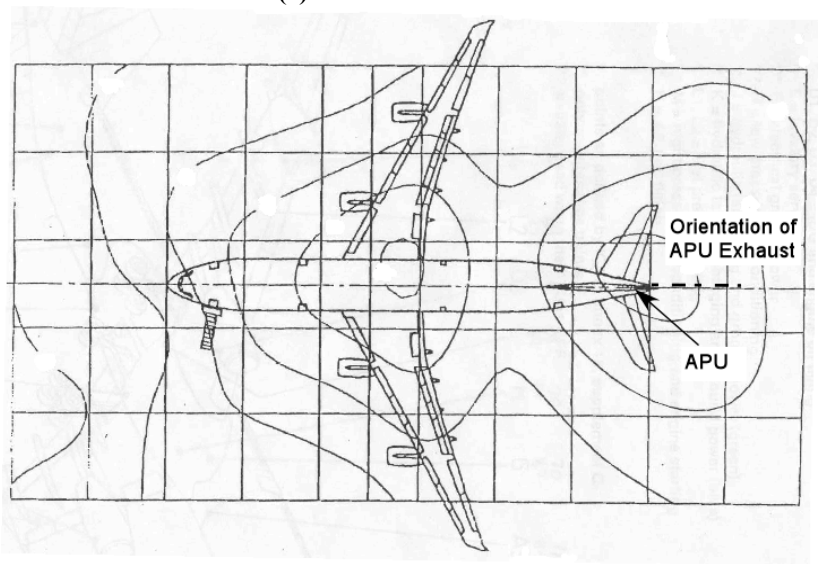

(b) Commercial aircraft

Figure 4. Measured ramp noise levels around two airplanes showing the influence of APU exhaust noise on overall noise levels, exhaust noise is loudest at angles near 60° from the tailpipe axis.

During the seventies and eighties, a good deal of research on combustion noise was done. Most of the investigations, however, were devoted to noise from open flames. Nevertheless, there were a number of significant contributions to combustion noise from turbofan engines. This is understandable. The simple reason is that open flame combustion noise experiments can be carried out in a standard laboratory. But for combustion noise from turbofan engines, a large test facility would be required.

Turbofan noise are dominated by jet and fan noise. Extracting combustion noise from full-scale engine noise measurements is not straightforward. This makes data acquisition and processing very challenging. An excellent exposition on combustion noise from turbofan engine may be found in a review by Mahan and Karchmer[1]. Semi-empirical prediction formulas for turbofan combustion noise intensity and the frequency at the spectral peak have been developed by a number of investigators including Mathews and Rekos[2] and Ho and Doyle[3]. Mathews and Rekos chose their empirical constants by best fit to the data measured at Pratt and Whitney. Ho and Doyle did the same but used GE data. Both prediction methods showed impressive agreement with their database. Recently at an AARC Core Noise Workshop, Krejsa[4] discussed the state of combustion noise prediction for turbofan engines. He compared predictions calculated by the method of Mathews and Rekos with GE data, in addition to Pratt & Whitney data and also predictions of the Ho and Doyle theory with Pratt & Whitney data, in addition to GE data. Krejsa pointed out that both methods gave poor agreement when used to predict outside their original database. This led him to conclude that not only present day prediction procedures needed improvement but also there was a lack of understanding of the noise source mechanism and transmission losses.

A fairly large body of publications on open flame combustion noise is available in the literature. Most of these works, except for the recent studies by Singh *et al.*[5,6], Rajaram and Lieuwen[7,8] were published before the mid-eighties. After that, there was almost a total absence of published work on the subject for more than a decade. What this means is that combustion noise has not benefited from recent advances in instrumentation and measurement techniques. A good summary of early experimental work on noise generated by open flame may be found in a review by Mahan[9]. In this review, the effects of burner geometry, flow rate, fuel equivalence ratio on overall sound power level are reported. Recently, Rajaram and Lieuwen[7] reported experimental results that confirmed the earlier finding of Kotake and Takamoto[10,11] and Mahan and Karchmer[1] that the spectral shape of open flame combustion noise was nearly universal. It is not affected by burner size and geometry, fuel consumption rate, flow velocity and turbulence intensity. However, the sound pressure level is much influenced by these parameters. Kotake and Takamoto found that an increase in burner diameter, flow velocity and turbulence level would lead to a corresponding increase in combustion noise. They also found that nozzle geometry had an effect on the sound pressure level with a rectangular nozzle producing more noise than a circular one. Extensive observations by various investigators had reported that the frequency at the spectral peak of open flame combustion noise lay in the range of 300Hz to 500Hz. Based on their experiments, Stephenson and Hassan[12] and Shivashankar *et al.*[13] suggested that this peak frequency was controlled by the kinetics of the combustion processes. It is, therefore, only affected by the fuel type used. Putnam[14], Kilham and Kirmani[15] and Petala and Petala[16] independently found through their own experiments that the total sound emission from flames scaled with heat release rate.

A number of studies reported the observation of power law dependence on frequency in the high frequency range of the noise spectrum. Abukov and Obrezkov[17] found a power law dependence with an exponent of –2·5 over the frequency range of 2 to 10 kHz. The same power law dependence was also observed by Billiard[18], Clavin and Siggia[19]. Clavin[20] theoretically predicted a combustion noise spectrum with –2·5 power law dependence on frequency. His theory made use of Kolmogorov scaling arguments and the assumption of a $k^{-5/3}$ inertial subrange velocity spectrum. However, the theoretical analysis of Huff[21] predicted a f^{-2} dependence.

The present investigation has two basic objectives. The first objective is to see if it is possible to identify clearly the combustion noise component in the noise spectrum of APUs. Since an APU noise spectrum consists of many noise components, it is not evident, at the outset, that this goal is attainable. The second objective is to study the characteristics of APU combustion noise. This also includes the development of scaling formula.

The rest of this paper is as follows. In Section 2, the experimental facility at Honeywell is described. A short description of the instrumentations used will be provided. Section 3 reports the procedure and the results of a data quality analysis. This is necessary as only high quality data would permit a clear and unambiguous identification of the combustion noise of an APU. In Section 4, the procedure by which combustion noise is identified is discussed and implemented. Comparison with open flame combustion noise spectrum is carried out as a part of the identification process. Section 5 reports some of the major combustion noise characteristics found in the present investigation. Finally, it will be reported in the conclusion section of this paper that the present study is unable to find evidence to support the existence of a second APU combustion noise mechanism.

II. Experimental Set-up

Assessment of uninstalled APU noise levels is critical for accurate prediction of installed levels around an airplane. All the noise data used in the present study were measured in the Honeywell APU test facility. The facility consists of an APU test cell specifically designed to isolate exhaust noise from inlet and case radiated noise to allow high quality source noise measurements. Shown in Figure 5, the enclosed cell has an opening in one wall through which the APU tailpipe extends. The wall is sealed around the tailpipe using two aluminum iris structures, one on each side of the 22-in thick wall, and bulk acoustic material is used to fill around the tailpipe in the axial space between the two iris. Outside the cell is a large concrete and asphalt pad. The wall of the cell extends 35 ft on either side of the tailpipe opening and 20 ft high.

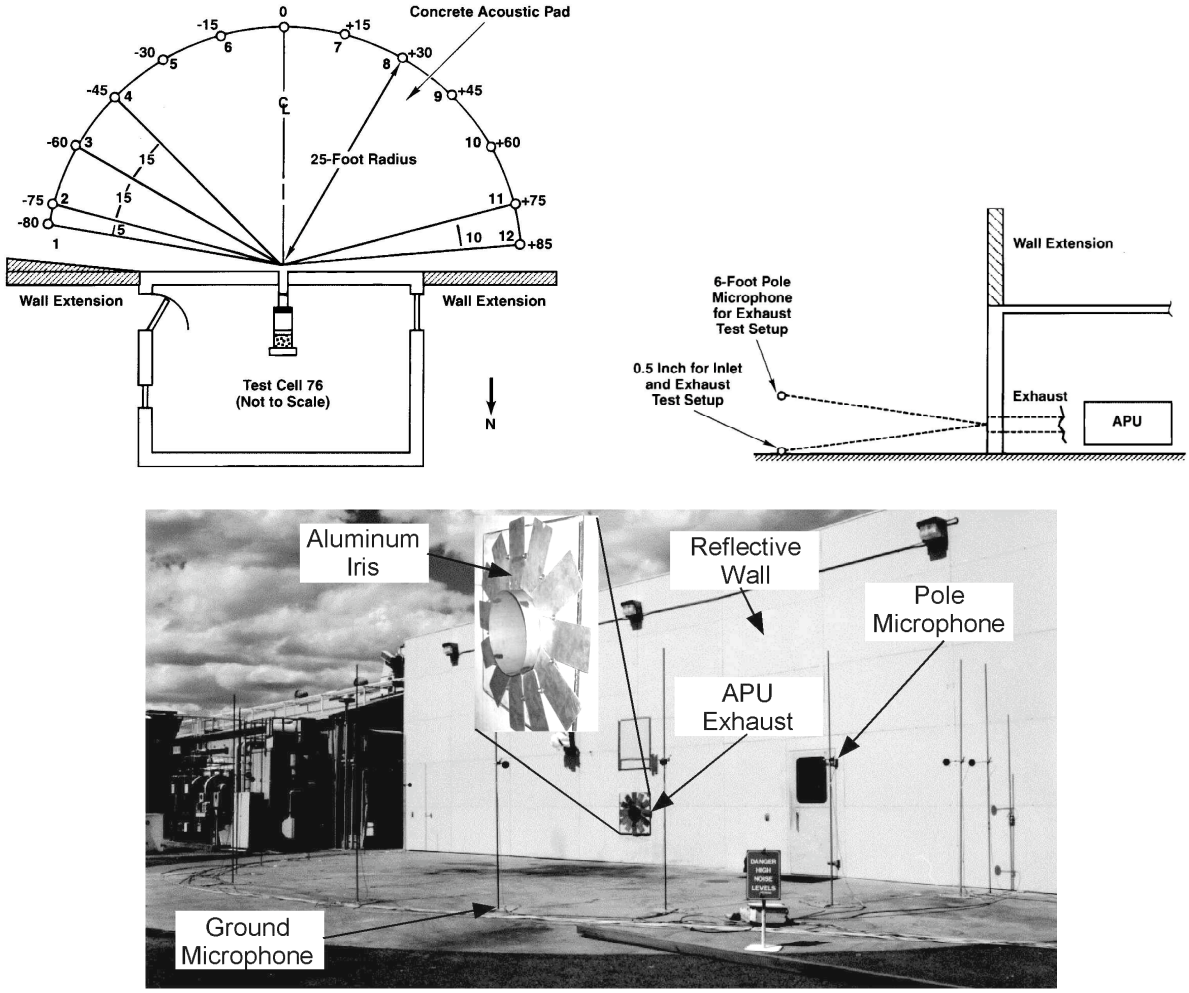

Figure 5. Honeywell test cell and microphone array for measurement of uninstalled APU exhaust noise.

Positioned around a 180° arc at a radius of 25 ft from the APU tailpipe exit are 24 microphones, 12 mounted on poles at a height of 6 ft and the other 12 beneath them on the ground. Both the pole and ground microphone signals are used to obtain free field sound pressure levels which are in turn used to calculate the exhaust sound power level and directivity spectra for engineering applications. Acoustic data acquisition equipment (the core of which is a 32-channel B&K Pulse system), is housed in a nearby trailer.

III. Data Quality Analysis

Narrow band noise data of 32 Hz bandwidth from three APUs are used in the present study. APU1 is a medium size APU. APU2 is the smallest. APU3 is the largest and has a combustion volume 1.12 times that of APU1 and 1.63 times that of APU2. Although the noise data of the three APUs were measured separately over a period of

time, the quality of the measured data is comparable. We will consider the noise data of APU1 as typical. We will first demonstrate that the data are of good quality.

The measured data, by design, have built-in redundancies. It is, therefore, possible to demonstrate by comparing measurements from different microphones that the data quality is reasonably good; taking into account the fact that these are engine noise data. This is important to the present study. The reason is that an APU has many sources of noise. Any measured spectrum contains the contributions from a multitude of noise components. Thus unless the data quality is high enough, a clear identification of a combustion noise component might not be possible.

A. Symmetry Test

The test facility (see Figure 5) is symmetric with respect to the centerline or the zero degree line. So a simple accuracy test of the measurements is to compare noise spectra measured by microphones located at the same angle to the left or the right of the plane of symmetry. Figure 6a shows a comparison of the noise spectra of APU1 at full power at θ=+75° and –75°. Figures 6b and 6c show similar comparisons at θ=±45° and ±15°. As can be seen, the two spectra in each of these figures are nearly identical especially for frequencies less than 800Hz. Figures 7a, 7b and 7c are similar comparisons of the measured noise spectra of APU1 at idle power. The spectra shapes are quite different from those of Figure 3. But again, there are good agreements between microphone measurements at equal angular positions from the plane of symmetry of the test facility.

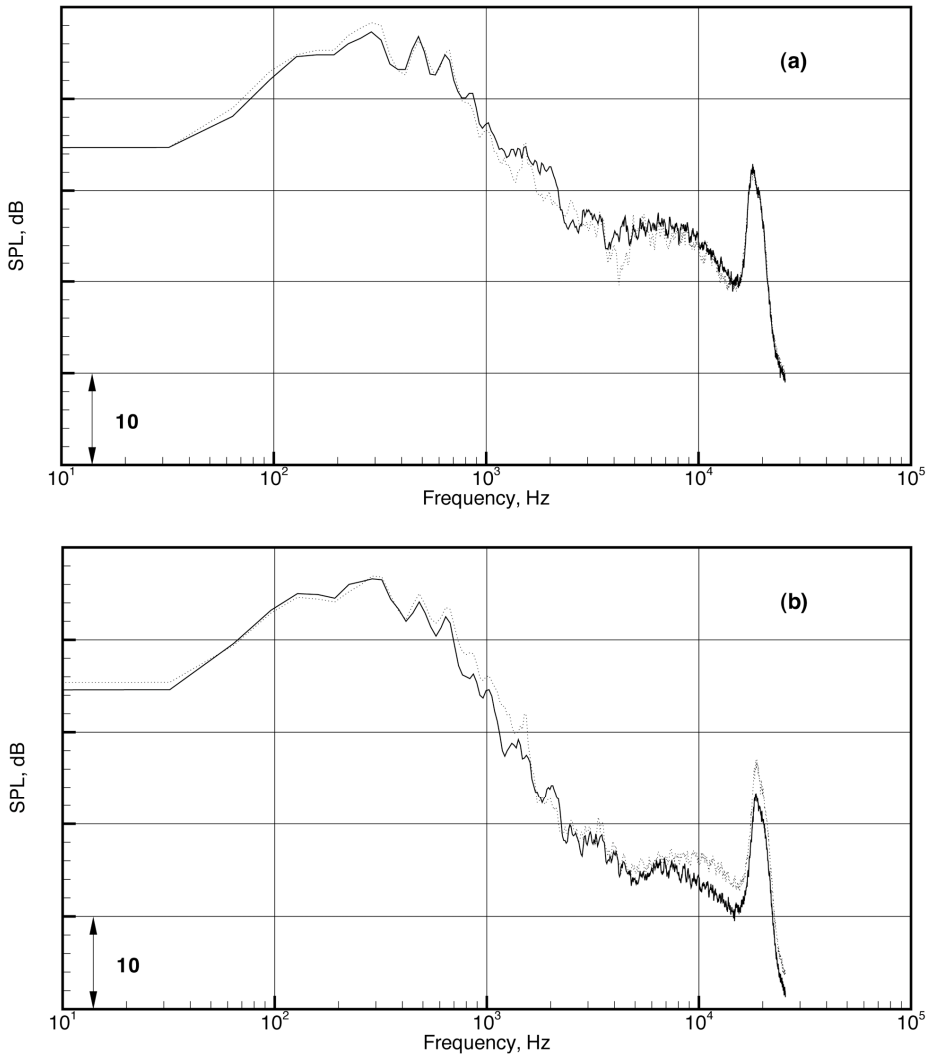

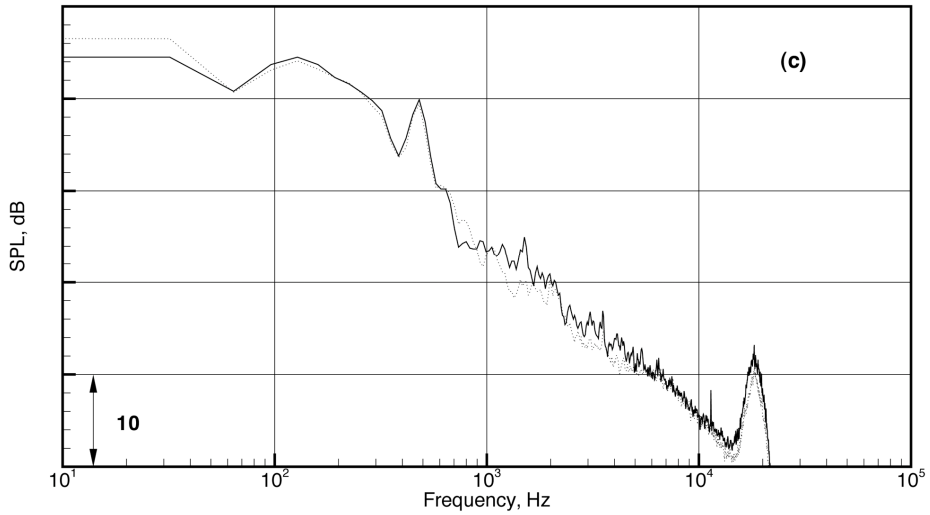

Figure 6. Comparison of noise spectra from APU1 at full power. Ground Microphone. (a) —— ϕ = 75°, ····· ϕ = –75°; (b) ϕ = 45°, ····· ϕ = –45°; (c) ϕ = 15°, ····· ϕ = –15°.

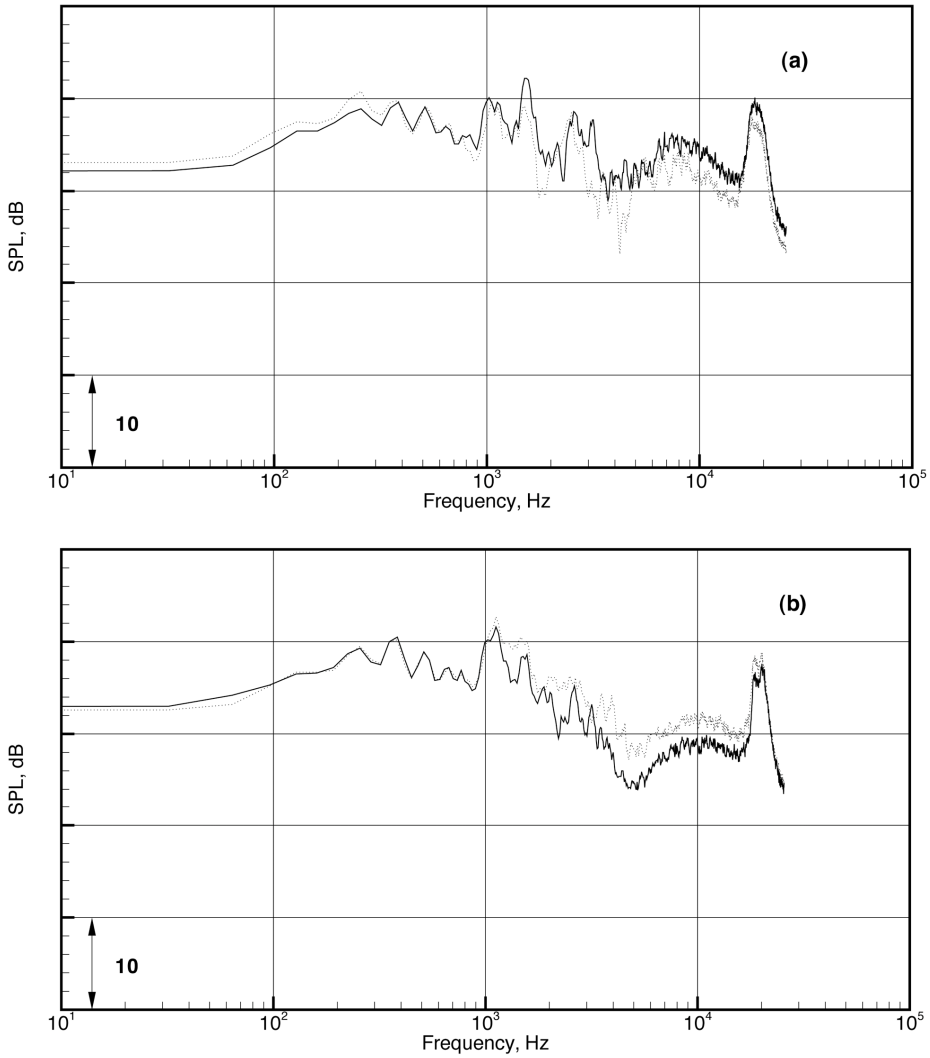

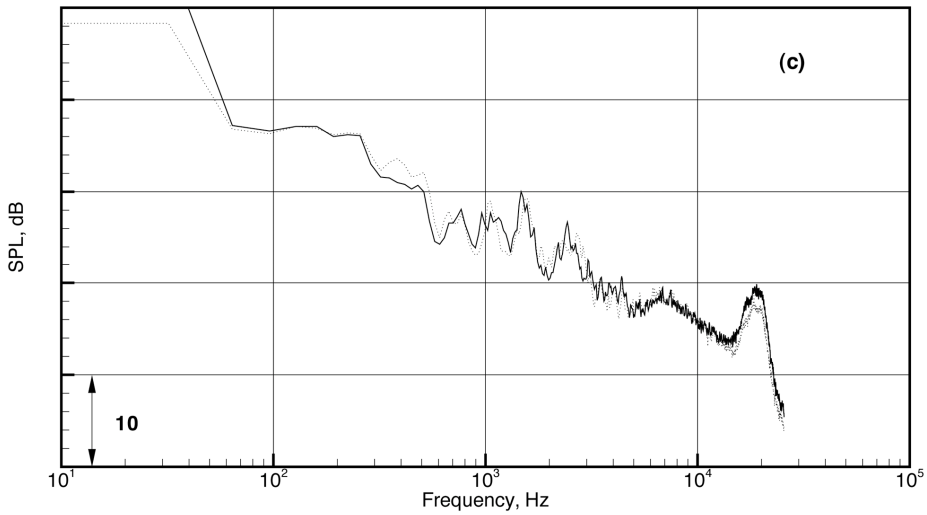

Figure 7. Comparison of noise spectra from APU1 at idle power. Ground Microphone.
(a) —— θ = 75°, ····· θ = –75°; (b) —— θ = 45°, ····· θ = –45°; (c) —— θ = 15°, ····· θ = –15°.

B. Comparisons between Pole and Ground Microphone Measurements

At each 15° angular position, noise is measured by a pole microphone at 6 feet above the concrete pad and by a ground microphone. This is shown schematically in Figure 8. The noise spectra measured by the pole and ground microphones are closely related. We will first establish quantitatively the exact relationship of the two sets of spectra. Then we will use this relationship to check the accuracy of the measurements.

As shown in Figure 8, sound radiated from the exhaust of an APU would be reflected off the concrete pad. The result is that the pole microphone receives sound radiated directly from the APU exhaust as well as that reflected off the concrete pad. Let us denote the pressure of the direct acoustic radiation by p and that reflected off the ground by $p_{\text{reflected}}$. Thus

$$p_{\text{pole}} = p + p_{\text{reflected}}. \tag{1}$$

We will use an overbar to represent ensemble or time average. By means of (1), the intensity of the pole microphone is given by

$$\overline{p_{\text{pole}}^2} = \overline{p^2} + \overline{p_{\text{reflected}}^2} + 2\overline{pp_{\text{reflected}}}. \tag{2}$$

It is to be noted that the difference between the distance traveled by the direct ray and the reflected ray is small compared to the distance of travel. A good approximation, therefore, is to take the wave propagation distance (hence the inverse distance squared) to be the same. This yields $\overline{p^2} \approx \overline{p_{\text{reflected}}^2}$.

Now it makes a significant difference whether the radiated sound is broadband and random or periodic and coherent. Because $p_{\text{reflected}}$ travels a longer path before reaching the pole microphone, there is a phase difference between it and the direct sound. For random broadband sound, the phase difference causes p and $p_{\text{reflected}}$ to be nearly uncorrelated so that

$$\overline{pp_{\text{reflected}}} \approx 0. \tag{3}$$

Hence for broadband noise, (2) becomes

$$\overline{p_{\text{pole}}^2} \approx \overline{p^2} + \overline{p_{\text{reflected}}^2} \approx 2\overline{p^2}. \tag{4}$$

This is the case for combustion noise. For tones or time periodic sound $\overline{pp_{\text{reflected}}}$ is not zero. It depends on frequency. At some frequencies p and $p_{\text{reflected}}$ have the same phase so that $\overline{pp_{\text{reflected}}} \approx \overline{p^2}$. At some other

frequencies p and $p_{reflected}$ are 180° out of phase. In this case, $\overline{pp_{reflected}} = -\overline{p^2}$. Therefore, for tones or time periodic sound,

$$0 < \overline{p_{pole}^2} \le 4\overline{p^2}. \tag{5}$$

For ground microphones, because of the surface doubling phenomenon, $p_{ground}=2p$. It follows,

$$\overline{p_{ground}^2} = 4\overline{p^2}. \tag{6}$$

Therefore, for combustion noise (4) and (6) give the following relationwhip between pole and ground microphone measurements,

$$\overline{p_{ground}^2} \ge 2\overline{p_{pole}^2}. \tag{7}$$

In other words, one would find,

$$\left[\begin{array}{c}\text{noise spectrum measured}\\ \text{by pole microphone}\end{array}\right] = \left[\begin{array}{c}\text{noise spectrum measured}\\ \text{by ground microphone}\end{array}\right] - 3\text{dB}. \tag{8}$$

Equation (8) provides a way to check the accuracy of the experimental measurements.

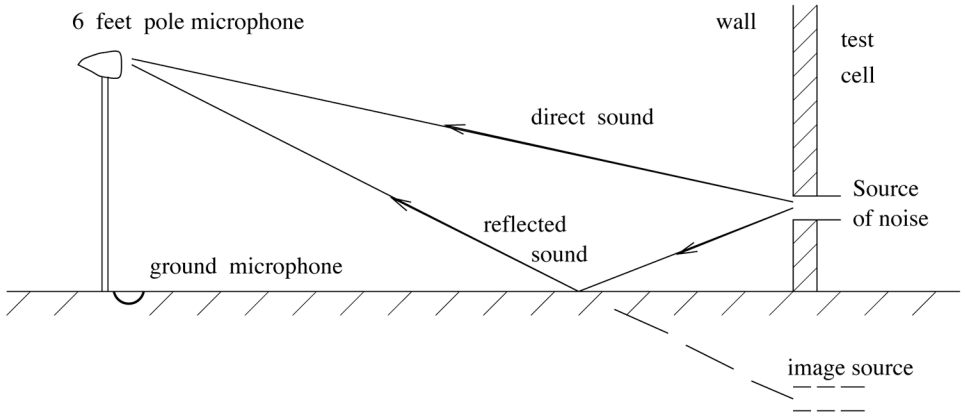

Figure 8. Pole and ground microphone measurements.

Figure 9a shows a superposition of the noise spectrum of APU1 measured by the 75° pole microphone at full power and the corresponding spectrum measured by the ground microphone minus 3dB. The pole microphone spectrum has deep valleys indicating noise cancellation between direct and reflected sound. Overall, if one overlooks these deep valleys, the envelopes of the two spectra are nearly the same. This indicates that the data must have been measured fairly accurately. Figures 9b and 9c show similar comparisons for the 45° and 15° pole and ground microphone measurements. As is evident, there are good agreements of the overall envelopes of the two sets of data. A similar data analysis has been performed for APU1 at idle power. The spectra are shown in Figures 10a, 10b and 10c. The noise spectra at idle power are distinctly different from those at full power. In all the cases, there are also good agreements between pole microphone noise spectra and those of the ground microphone after subtracting 3dB. Based on the results of both the symmetry test and the pole versus ground microphone data comparisons, we believe that the measured APU noise data are reliable and accurate.

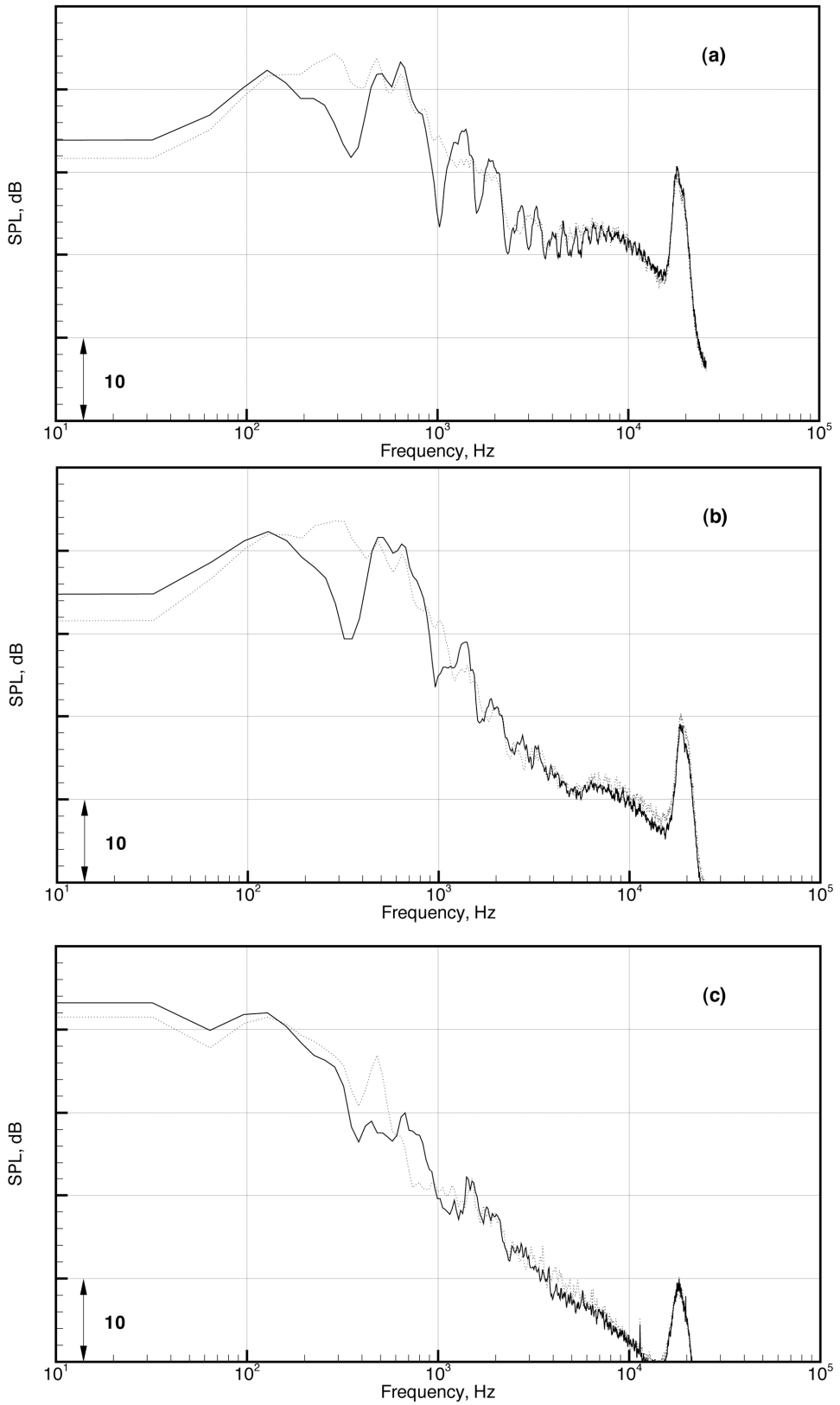

Figure 9. Comparison of noise spectra from APU1 measured by pole and by ground microphones at full power. ——— pole mic.; ····· ground mic. –3.0dB. (a) θ = 75°, (b) θ = 45°, (c) θ = 15°.

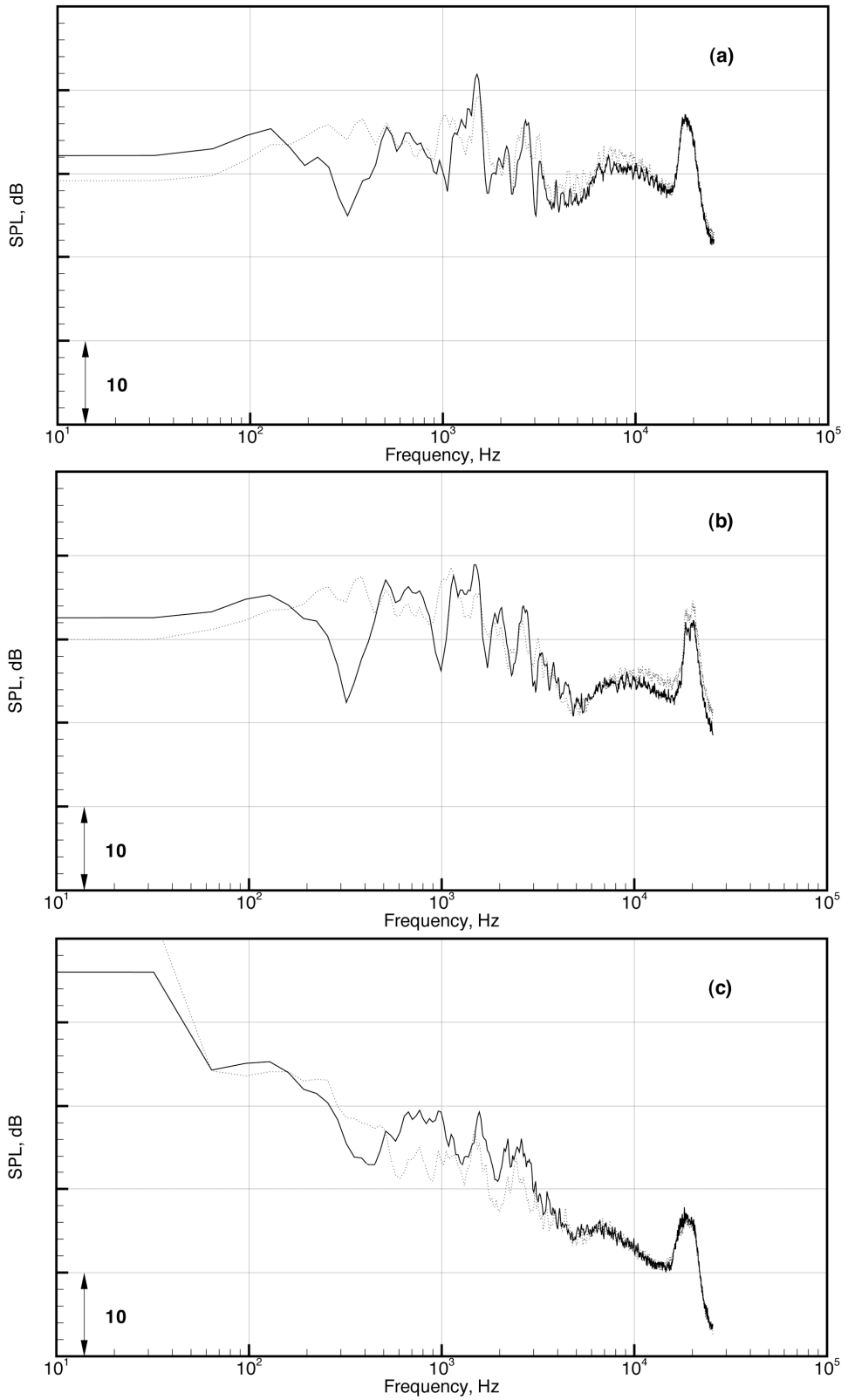

Figure 10. Comparison of noise spectra from APU1 measured by pole and by ground microphones at idle power. —— pole mic.; ····· ground mic. –3.0dB. (a) □ = 75°, (b) □ = 45°, (c) □ = 15°.

IV. Identification of Combustion Noise from APUs

A number of investigators[1,7,8,10,11] in the past had suggested that combustion noise had a unique spectral shape, even though the frequency and sound pressure level at the peak of the spectrum were affected by a multitude of flow and geometrical variables such as turbulence intensity, fuel consumption rate, geometry of burner, equivalence ratio, and flame temperature. The situation is very similar to the mixing noise problem of high-speed jets. Tam, Golebiowski and Seiner[22] analyzed a very large set of jet noise data measured at the Jet Noise Laboratory of the NASA Langley Research Center. They found empirically that all the spectra of noise radiating to the downstream direction of the jet, regardless of jet Mach number and temperature ratio, invariably, have the shape of a similarity spectrum. This spectral shape, labeled as the large turbulence structures noise spectrum, is shown in Figure 11. The frequency and sound pressure level at the peak of the spectrum, on the other hand, are very much dependent on jet Mach number, jet temperature ratio and direction of radiation. Simultaneously, they found that all the measured noise spectra, radiating to the sideline, regardless of jet Mach number and temperature ratio, invariably, have the shape of another similarity spectrum. This spectrum, which they attributed to being the noise from the fine scale turbulence of the jet flow, is also shown in Figure 11. For noise spectra radiating to angular directions in between the sideline and downstream direction around the jet axis, they were found to fit a combination of the two similarity spectra. Tam, Golebiowski and Seiner[22] provided the following analytical spectral shape formula for the large turbulence structures noise,

$$10\log F = \begin{cases} -5.64174 - 27.7472\log\left(f/f_p\right), & f/f_p \geq 2.5 \\ -\left\{1.06617 - 45.2994\log\left(f/f_p\right) \right. & \\ \quad \left. +21.40972\left[\log\left(f/f_p\right)\right]^2\right\}\cdot\log\left(f/f_p\right), & 2.5 \geq f/f_p \geq 1 \\ -38.19338\left[\log\left(f/f_p\right)\right]^2 - 16.91175\left[\log\left(f/f_p\right)\right]^3, & 1 \geq f/f_p \geq 0.5 \\ -2.53895 + 18.4\log\left(f/f_p\right), & 0.5 \geq f/f_p \end{cases} \quad (9)$$

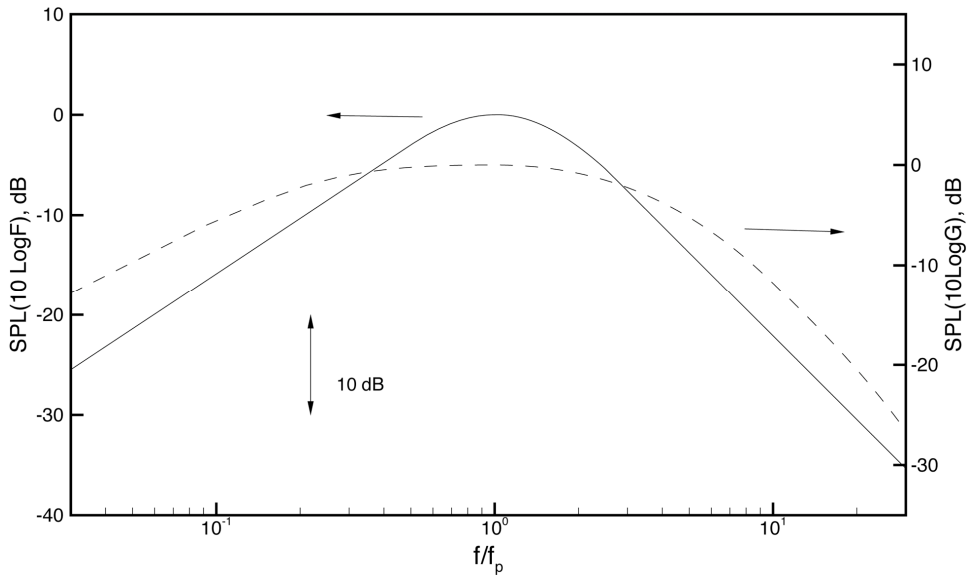

Figure 11. Similarity spectra for the two components of turbulent mixing noise: ——— large turbulence structures/instability waves noise, and – – – fine-scale turbulence noise.

The two similarity spectra of Tam, Golebiowski and Seiner were subsequently found to fit noise spectra of coaxial jet by Dahl and Papamoschou[23], of non-axisymmetric jets by Tam[24] and Tam and Zaman[25]. In the hands of Vishwanathan[26,27] the similarity spectra were even used as a jet noise diagnostic tool.

In the present study, we follow the strategy of Tam, Golebiowski and Seiner. The first step is to identify if there is, indeed, a unique spectral shape for the combustion noise of APU. This is to be followed by extensive demonstration that the spectral shape, indeed, fits all measured APU noise spectra. It did not take long to find that

the spectral shape of formula (9) was also the spectrum for combustion noise. This is totally unexpected. However, as we will show below, this is true regardless of the direction of radiation, the operating power level of the engine and the size of the engine.

To demonstrate this very unexpected finding, we will begin by comparing formula (9) with the noise spectra of APU1 and then APU2 and APU3. Since combustion noise is most intense at full power, we will start at the highest power setting. Figure 12 shows comparisons of similarity spectrum (9) and measured noise of APU1 at high power in the 75°, 45° and 15° directions. It is readily seen that there is a good fit to the experimental data in each case. It is important to emphasize that the observed noise peak in these figures are not from the exhaust jet of the APU. First of all, the jet velocity is too low to generate the level of noise measured. In addition, noise spectrum (9) called the large turbulence structures noise similarity spectrum, only fits jet noise data in the downstream direction. Jet noise in the sideline direction such as 75° fits only the broad spectrum of fine scale turbulence noise of Figure 11. There is, therefore, no question that the spectral peaks in Figure 12 are from combustion noise.

Figure 13 shows the measured noise spectra of APU1 operating at mid-power. Shown also is the similarity spectrum of formula (9). As can be seen, there is good agreement between the shape of the similarity spectrum and measurements. Figure 14 shows the noise spectra of APU1 at low power. At low power, the combustion noise intensity is low. At the same time, turbomachinery noise of the APU is much higher. As a result, it is somewhat difficult to pinpoint the combustion noise component in the measured spectrum. To assist in identifying combustion noise, the noise spectrum at high power at the same angular direction (displaced appropriately to a lower level) is also plotted in Figures 14a, 14b and 14c. The overlapping part of the spectra indicates where the combustion noise is.

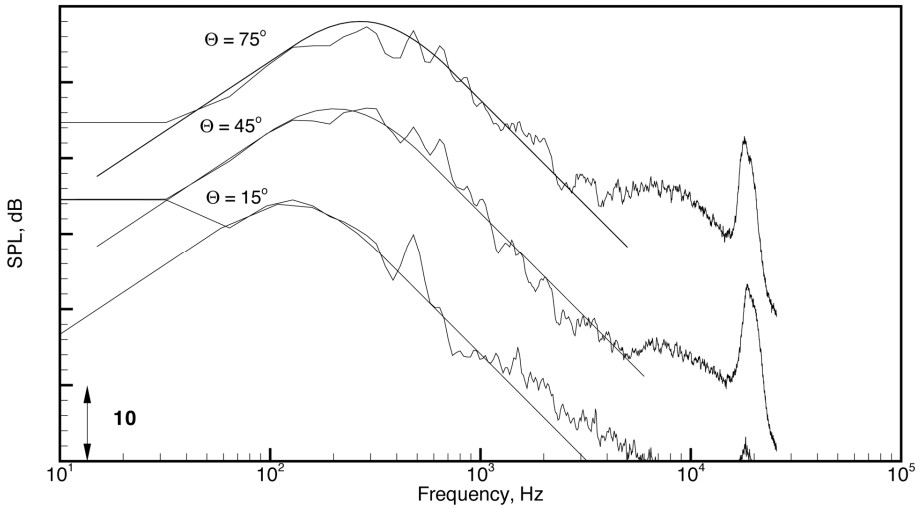

Figure 12. Noise spectra of APU1 at full power. Spectra displaced vertically by 10dB. Ground microphone.

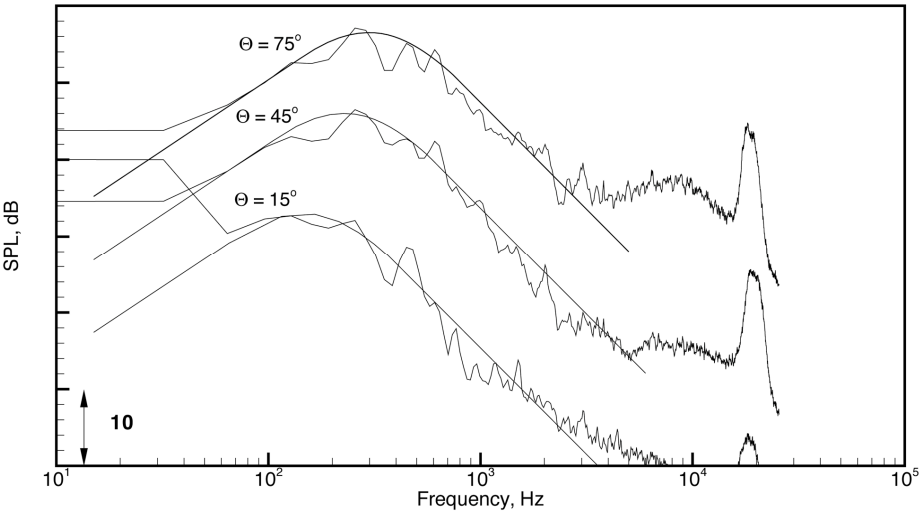

Figure 13. Noise spectra of APU1 at mid-power. Spectra displaced vertically. Ground microphone.

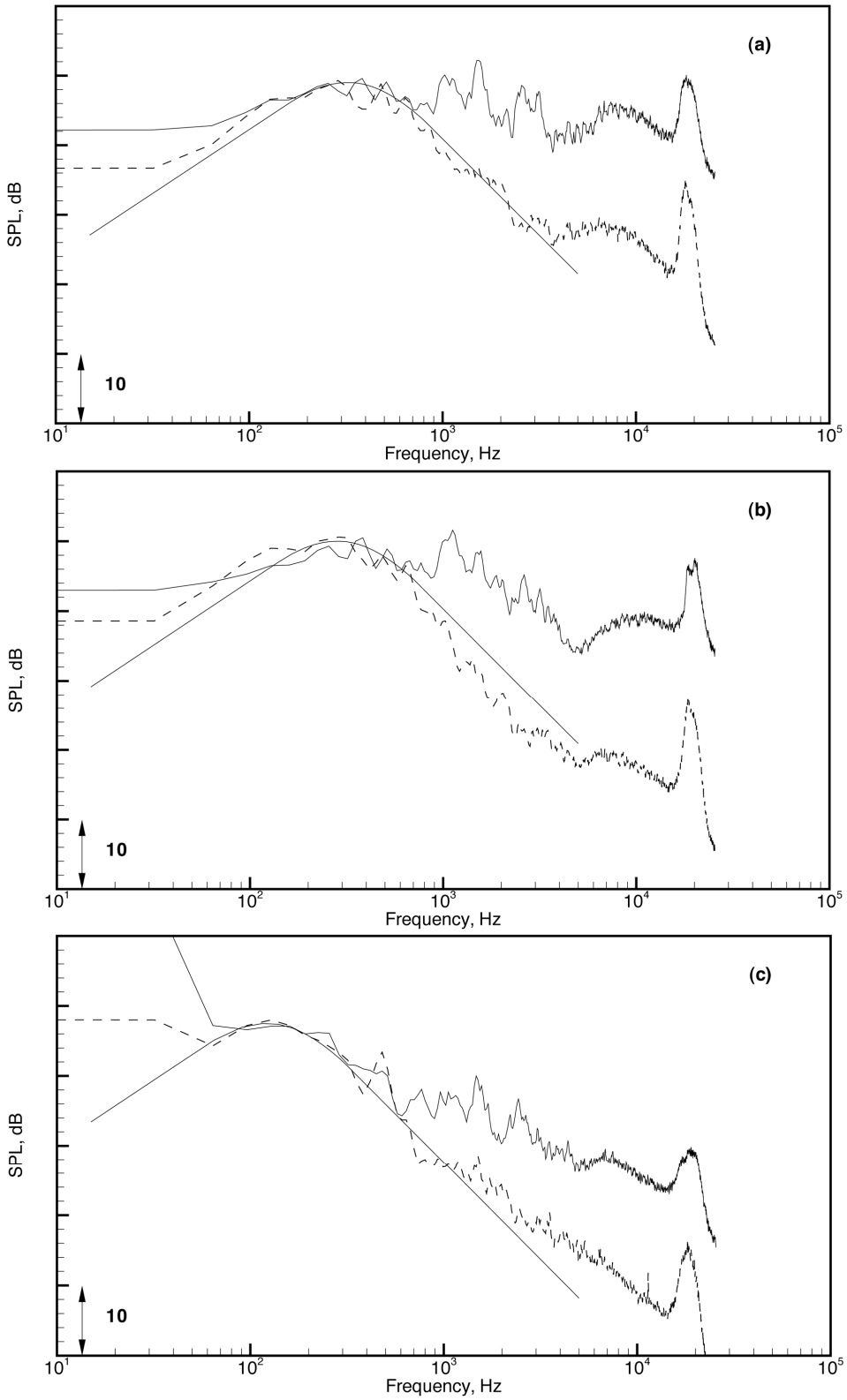

Figure 14. Noise spectra from APU1 at low power. Ground Microphone.
(a) □ = 75° —— low power, – – – full power –8.0dB;
(b) □ = 45° —— low power, – – – full power –6.0dB;
(c) □ = 15° —— low power, – – – full power –6.5dB;

Figure 15, 16 and 17 show similar noise spectra of APU2. Shown also is the similarity spectrum. It is readily seen that similarity spectrum (9) is, indeed, a good fit to the data. It turns out for this small engine, the combustion noise is still the dominant noise component at low power. This is shown in Figure 17. Figures 18, 19 and 20 are noise spectra of APU3. For this large APU, the noise spectra appear to have low frequency contamination. We are unable to identify the source of the very low frequency noise to the left of the peak of the combustion noise.

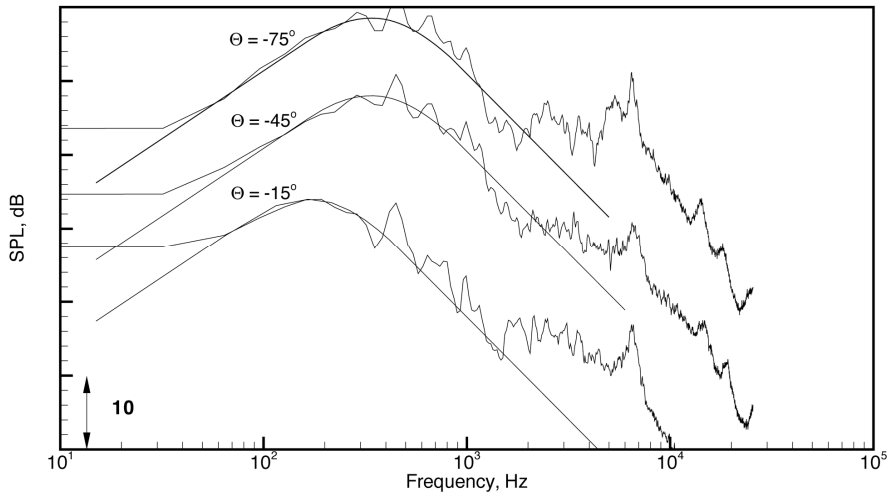

Figure 15. Noise spectra of APU2 at full power. Spectra displaced vertically. Ground microphone.

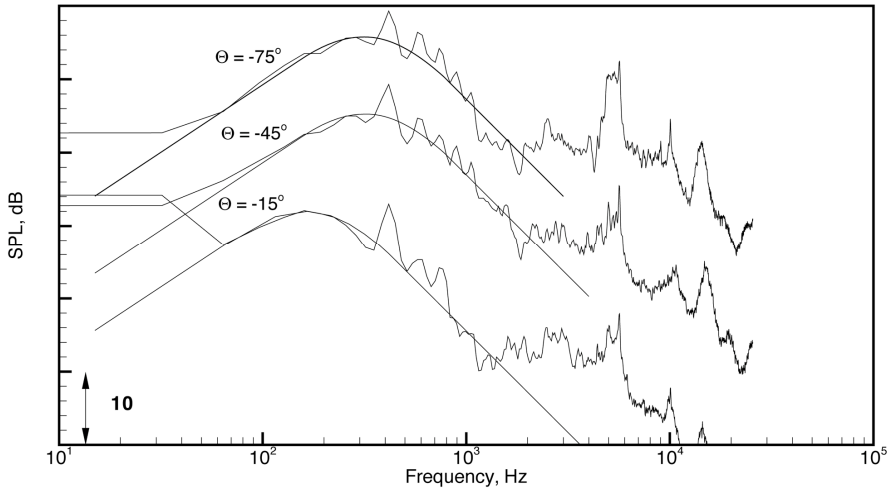

Figure 16. Noise spectra of APU2 at mid-power. Spectra displaced vertically. Ground microphone.

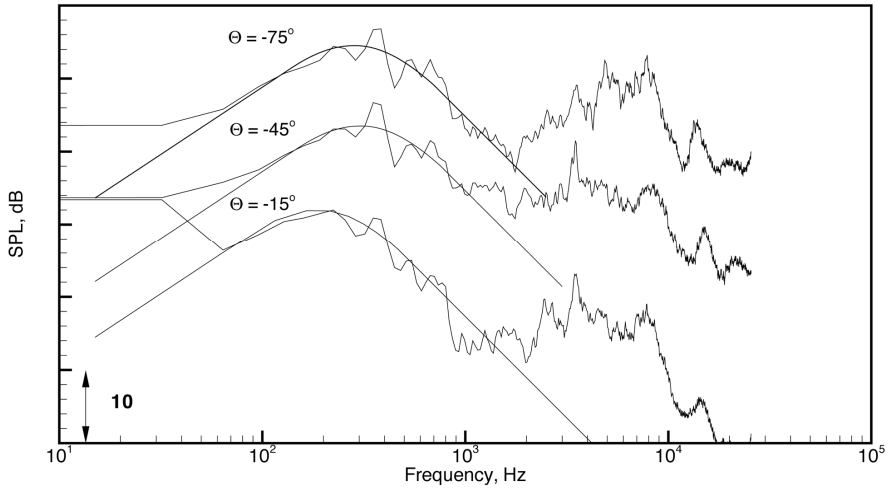

Figure 17. Noise spectra of APU2 at low power. Spectra displaced vertically. Ground microphone.

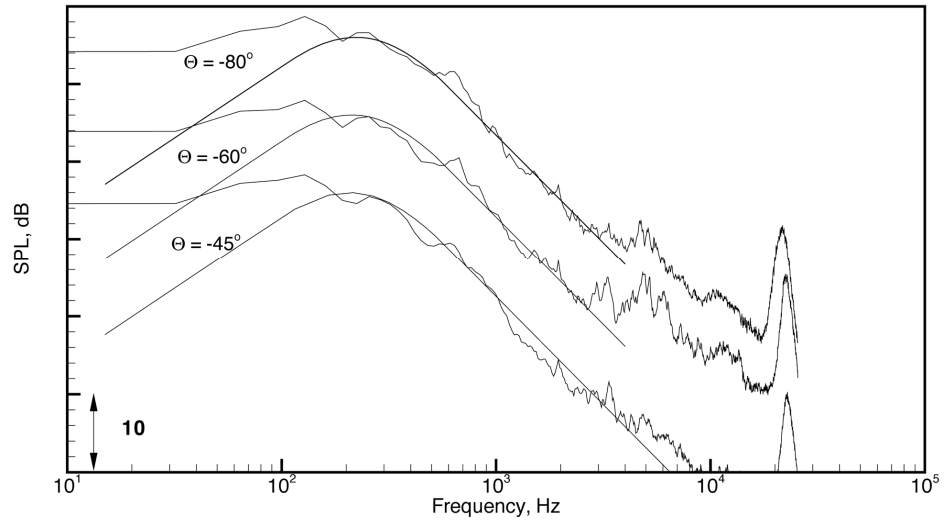

Figure 18. Noise spectra of APU3 at full power. Spectra displaced vertically. Ground microphone.

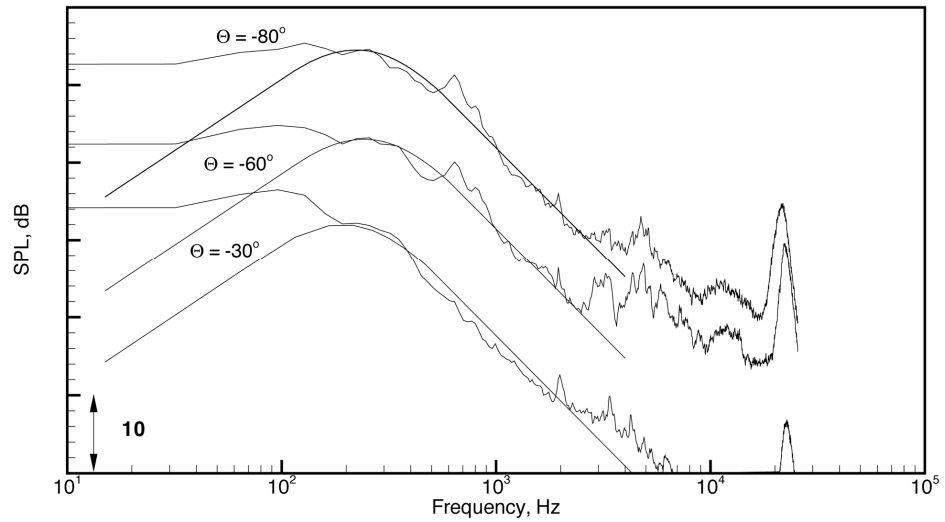

Figure 19. Noise spectra of APU3 at mid-power. Spectra displaced vertically. Ground microphone.

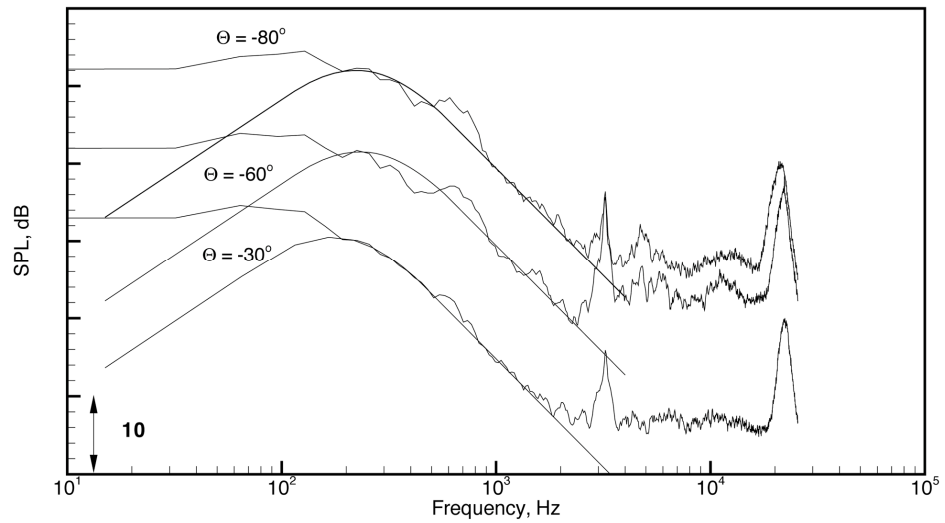

Figure 20. Noise spectra of APU3 at low power. Spectra displaced vertically. Ground microphone.

It is appropriate to point out that Figures 12 to 20 show the noise spectra of three APUs operating at three power settings. In each case, the spectral shape of the combustion noise component compare well with similarity spectrum (9) in all directions of radiation. It is our assessment that within the experimental accuracy of the data, there is good agreement overall. It is, therefore, appropriate to regard similarity spectrum (9) to be the unique noise spectral shape of APU combustion noise. Of course, this conclusion should be further verified using other APU data in the future.

In the literature, there are published combustion noise data from turbofan engines. However, most of them; e.g., Mahan and Karchmer[1] are given in 1/3 octave band, not narrow band. There is a large loss of resolution in converting 1/3 octave band spectrum to narrow band spectrum. As a result, it is difficult to test how they compare with similarity spectrum (9). Other than turbofan noise data, there is a large body of open flame combustion noise data. Again, we have not been able to find good quality narrow band data except for the recent work of Rajaram and Lieuwen[7]. Open flame combustion noise data are measured in controlled laboratory conditions. Not only the data quality could be high, but also the noise spectrum is unlikely to be contaminated by extraneous noise as is the case of outdoor engine noise measurement. Figure 21 shows comparisons of three noise spectra measured by Rajaram and Lieuwen and similarity spectrum (9). The spectra were measured in the 90°, 70° and 50° directions. The data does not extend to frequencies below 100Hz. For this reason, it is only possible to test the high frequency half of the similarity spectrum. The good agreement provides support for the contention that the spectral shape of the combustion noise is independent of the size of the combustion chamber; an open flame experiment may be regarded as in an infinite size combustion chamber.

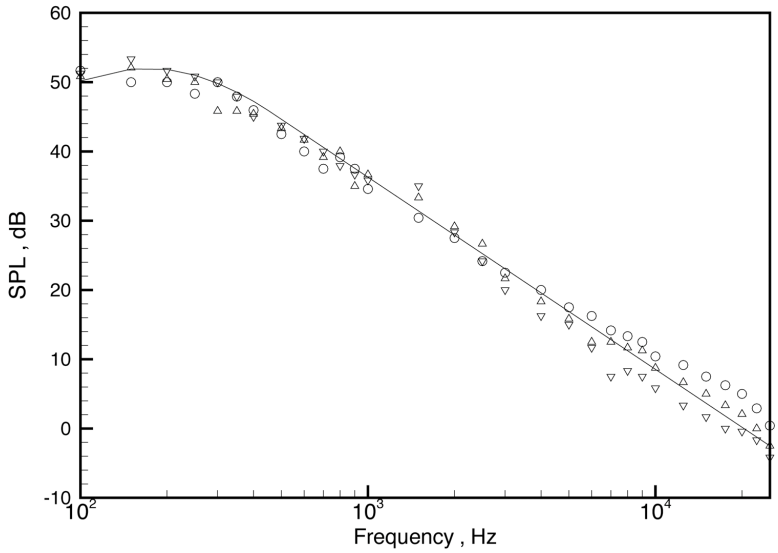

Figure 21. Comparison of noise spectra from open flame burner [7] and similarity spectrum. O 90°, □ 70°, ▽ 55°.

V. Characteristics of APU Combustion Noise

We will now accept the proposition that APU combustion noise has a nearly unique spectral shape given by formula (9). With the shape of the spectrum defined, combustion noise is completely characterized by just two parameters. They are the frequency and sound pressure level at the peak of the spectrum. For convenience, we will refer to them as the peak frequency and peak level. Of interest to us is how these two parameters are influenced by the operating power level, engine size, direction of radiation and fuel consumption rate. In all the engine tests, jet A fuel was used. So we are unable to study the variation of these parameters with fuel type.

A. Variation of Peak Level and Peak Frequency

Figure 22 shows the variation of peak level with respect to the direction of radiation for APU1 at all three power settings. The levels plotted are the peak of the fitted similarity spectra. They are subjected to a probable error of 1.5dB. As can be seen, except for low angles, the peak level is near constant. This is true for all power settings. Figures 23 and 24 show similar plots for APU2 and APU3. Again, the peak level, regardless of power setting, remains nearly constant in every case except at low angles. One probably explanation for the dip in peak level at low angles is the presence of a low speed hot jet exhausting from the tailpipe of the APU. The jet spreads out in the flow

or the zero degree direction. The jet, being hot, tends to cause strong refraction of sound wave away from the jet flow direction. This leads to a reduction of noise radiating to the low angles. It is known for high-speed jet noise, this same mean flow refraction effect is responsible for the creation of a relative cone of silence, around the jet flow direction, for fine scale turbulence noise[28].

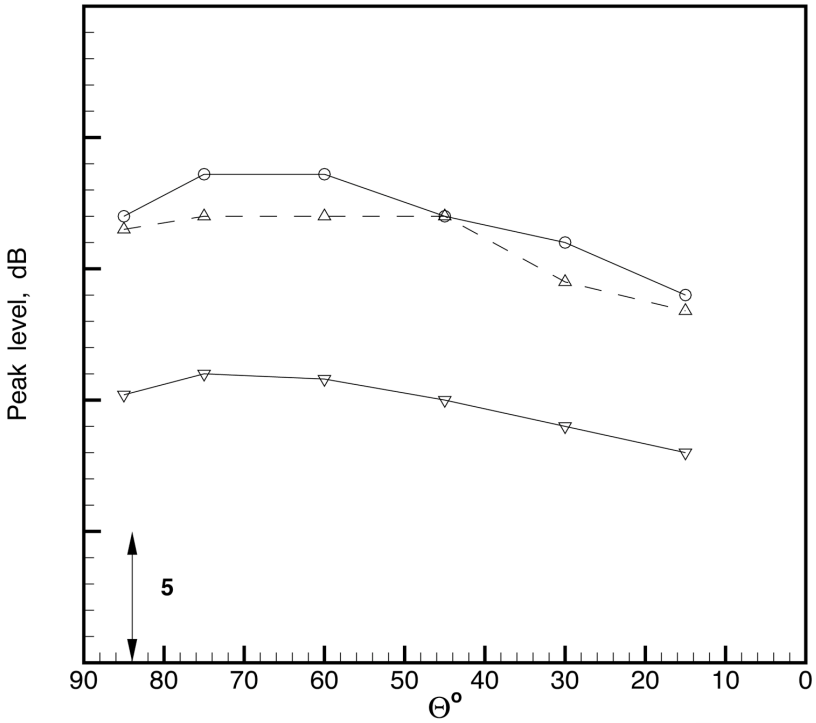

Figure 22. Directivity of peak noise level. APU1. Ground microphone. O high power, □ mid-power, ∏ low power.

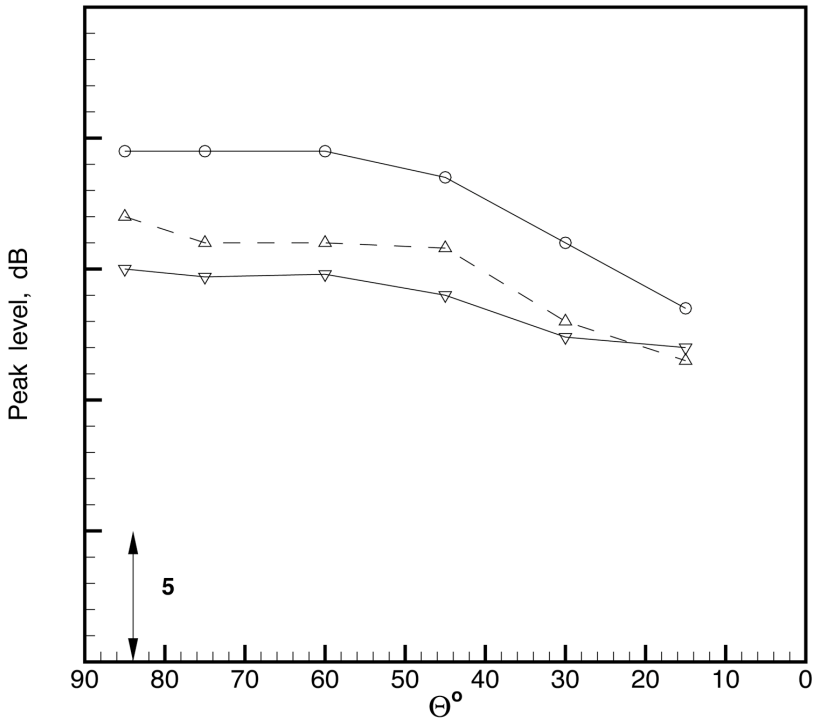

Figure 23. Directivity of peak noise level. APU2. Ground microphone. O high power, □ mid-power, ∏ low power.

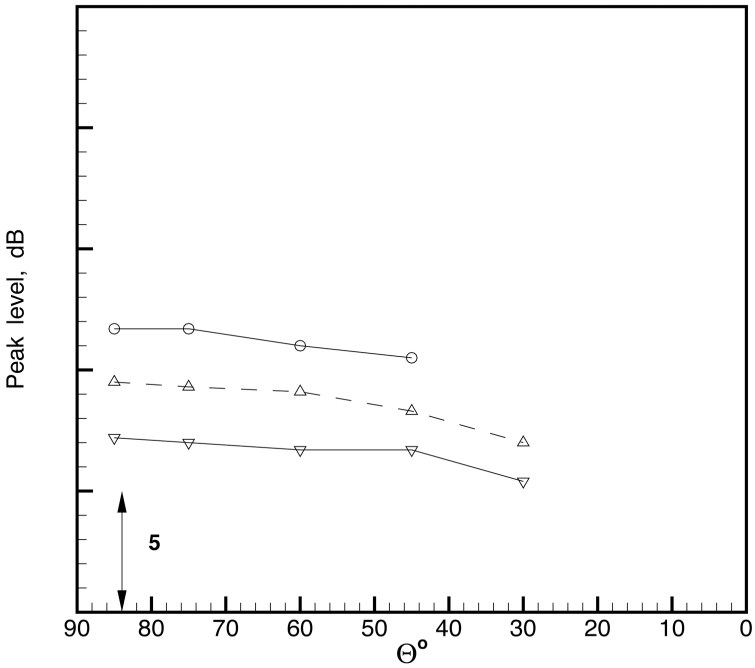

Figure 24. Directivity of peak noise level. APU3. Ground microphone. O high power, □ mid-power, ∩ low power.

Figure 25 shows the variation of the peak frequency of combustion noise from APU1 at high, middle and low power settings with direction of radiation. Probable error of the measurements is around 30Hz. It is evident that the peak frequency is quite constant again except at low angles. There appears to be a systematic small increase in peak frequency with engine power level. The average peak frequency (high angles) increase from about 250Hz to 300Hz when power level reduces from high to low. Figure 26 shows similar plots for APU2. Again the peak frequency is nearly a constant for high angles for each power setting. However, the average peak frequency, unlike that of APU1, decreases with decrease in engine power level. The average peak frequency at peak power is around 350Hz and drops to around 300Hz at low power. Figure 27 contains peak frequency plots for APU3. In this case, the average peak frequency is nearly the same for both the high and low power settings with mid-power the highest.

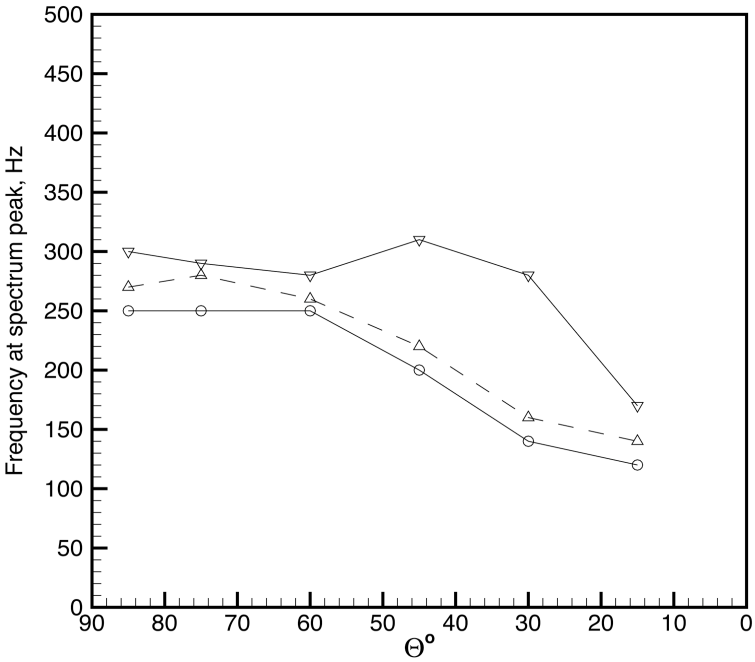

Figure 25. Variation of frequency at spectrum peak with direction of radiation. APU1. Ground microphone. O high power, □ mid-power, ∩ low power.

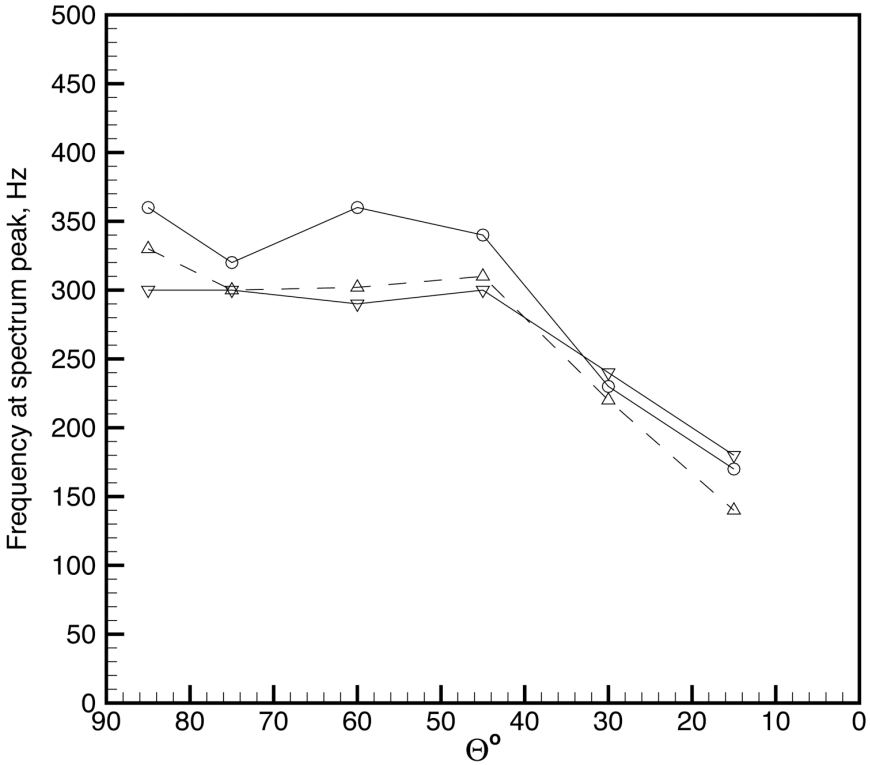

Figure 26. Variation of frequency at spectrum peak with direction of radiation. APU2. Ground microphone. O high power, □ mid-power, △ low power.

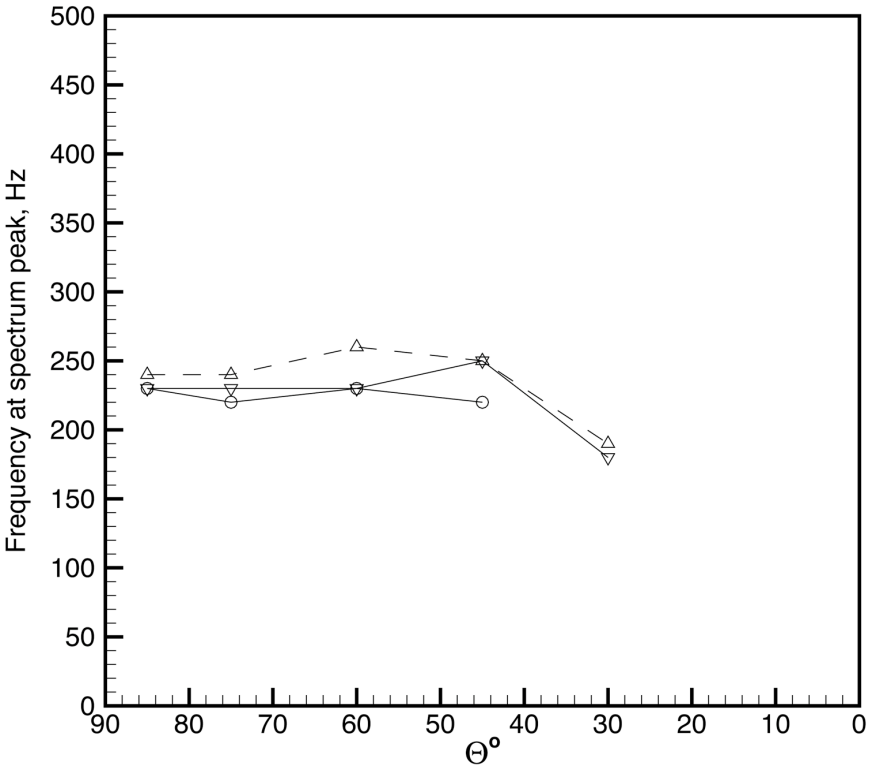

Figure 27. Variation of frequency at spectrum peak with direction of radiation. APU3. Ground microphone. O high power, □ mid-power, △ low power.

Based on the above observations, it is possible to conclude that the peak frequency of APUs is around 250 to 350Hz. It is fairly constant but drops to a lower value at low angles. The reason for the lower frequency is probably the result of mean flow refraction by the low speed hot jet exhausting from the APU. It is well known that high frequency sound undergoes more refraction than low frequency sound. Thus one expects the noise spectrum to undergo a shift to low frequencies in directions near the zero degree line. There is no systematic variation of the peak frequency with engine power settings. It appears that it is a function of engine designs. Further study of this dependence is necessary and beneficial.

B. Effect of Fuel Consumption Rate

The intensity of combustion noise radiated to the far field from an APU is equal to the noise intensity generated by combustion in the combustion chamber modified by the transmission loss due to propagation through the turbine and ducting until the sound reaches the end of the tailpipe of the APU. Symbolically, we may write,

$$\begin{bmatrix}\text{Noise intensity at}\\ \text{a far field microphone}\end{bmatrix} = \begin{bmatrix}\text{Noise intensity inside}\\ \text{combustion chamber}\end{bmatrix} \begin{bmatrix}\text{Transmission}\\ \text{loss}\end{bmatrix} \frac{1}{r^2} \tag{10}$$

where r is the distance from the APU tailpipe exit to the microphone.

Fuel efficiency for APUs is nearly 99%. In other words, fuel is completely consumed. The noise (pressure fluctuations) produced by combustion must be proportional to the rate of heat released in the combustion process. Thus, if Q is the fuel consumption rate for APUs operating at 100% fuel efficiency, the noise intensity in the combustion chamber must be proportional to Q^2. The transmission loss of an APU depends critically on its design. However, for the same APU, the transmission loss, to a good approximation, is independent of power setting. It follows from (10), for a particular APU, the noise intensity, I, radiated to a far field microphone must vary with Q^2; i.e.,

$$I_{\text{far field}} \propto Q^2. \tag{11}$$

(Note: the proportionality constant of (11) varies from APU to APU)

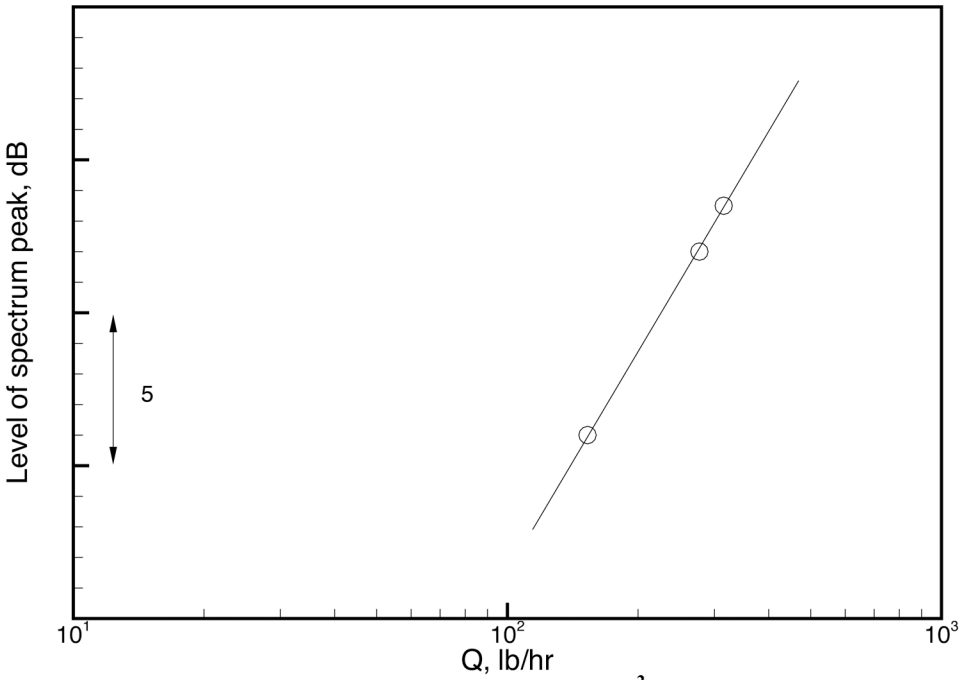

Figure 28. Comparison of scaling formula $I \sim Q^2$ with data. APU1.

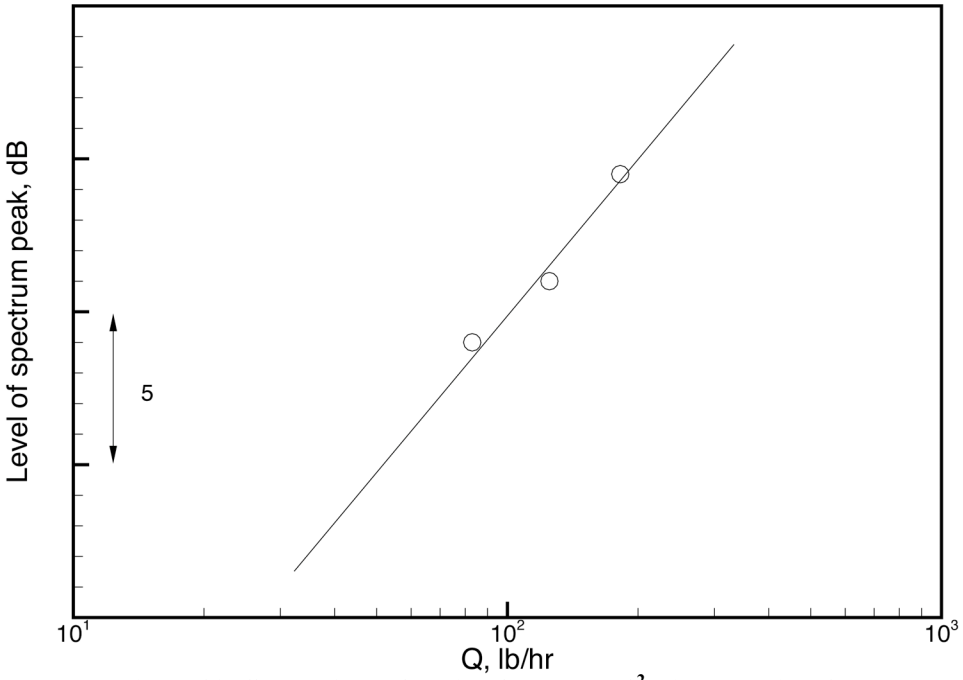

Figure 29. Comparison of scaling formula $I \sim Q^2$ with data. APU2.

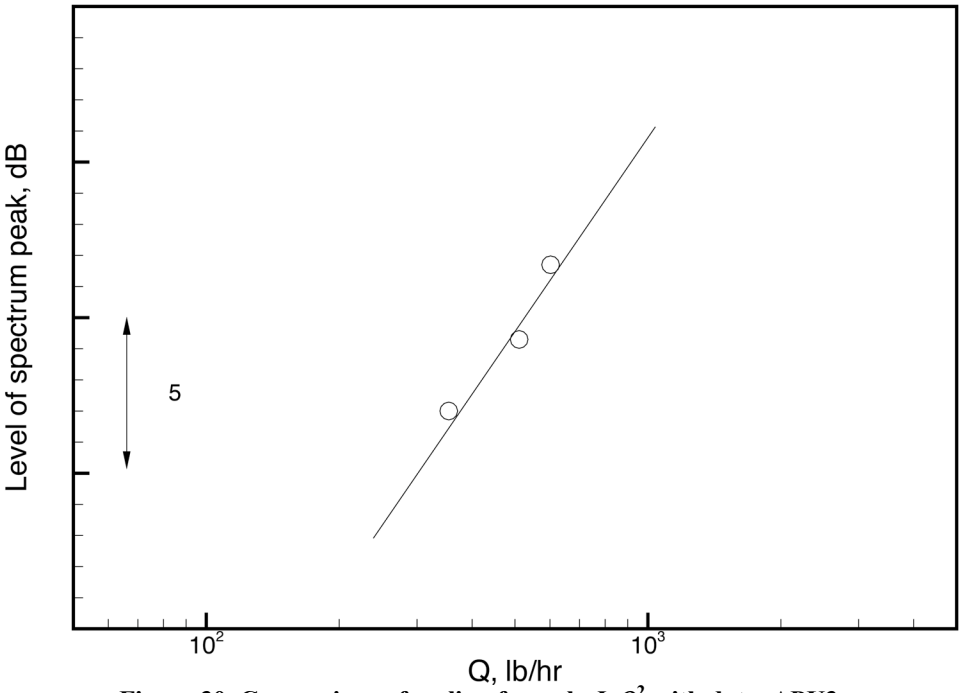

Figure 30. Comparison of scaling formula $I \sim Q^2$ with data. APU3.

The validity of scaling formula (11) may be tested. Figure 28 shows the relative peak noise level of APU1 measured by the 75° ground microphone as a function of fuel consumption rate, Q, in 1b/hr. Plotted in the figure also is the line $I_{\text{far field}} \propto Q^2$. There is a fair agreement between the measured data and scaling formula (11). Figures 29 and 30 show similar comparisons for combustion noise from APU2 and APU3. Again, on taking into consideration of the probable error of the data, the agreement appears to be reasonable. We believe that, until a more quantitative prediction formula is developed, scaling formula (11) may be used to provide a first estimate of the sound intensity of an APU at different power level.

VI. Conclusion

In this paper, we have presented extensive experimental measurements to demonstrate that combustion noise from APUs has a unique spectral shape. The spectral shape is the same regardless of engine design, power setting and directivity. The spectral shape is the same as the similarity spectrum of large turbulence structures noise of high-speed jets found by Tam, Golebiowski and Seiner[22]. An obvious question then is whether combustion noise of APUs is, in any way, related to the large turbulence structures of the combustion flame. We have given this question a considerable amount of attention. However, so far no compelling evidence has been found to relate combustion noise to large turbulence structures of flame or flow. This is an open question and needs further investigation.

The present study finds that the peak frequency of APU combustion noise generally lies in a narrow frequency band between 250 to 350Hz. No systematic frequency variation within this range has been found. It appears that engine design has a significant influence on how different engine operating parameters affect the peak frequency. Peak level of APU combustion noise, except at low angles, has a nearly uniform directivity. For a given APU, the peak level varies in proportion to the square of the fuel consumption rate. To scale noise level for APUs of different design is not possible at this time. More work is required before this possibility may be realized.

In the literature, there are suggestions that combustion noise may be generated by a second mechanism in addition to directly from the combustion process. This is the hot spot theory. This theory assumes that hot spots or entropy waves are formed downstream of the flame. Analysis was provided to show significant noise generation as these hot entropy spots pass through a nozzle or a constriction. In the present investigation, a very large set of data was examined to see if there was, indeed, a second component of combustion noise. So far none have been found. We are of the opinion that, perhaps, APUs do not generate a second component of combustion noise.

Acknowledgment

The work was initiated during a visit by the first author to Honeywell. The visit was supported by the Industrial Visit Program of the Aeroacoustics Research Consortium.

References

1. J.R. Mahan, A. Karchmer, Combustion and core noise in *Aeroacoustics of Flight Vehicles: Theory and Practice* ed. H.H. Hubbard, NASA RP-1258, pp. 483–516 (1991)
2. D.C. Mathews, N.F. Rekos,Jr., Prediction and measurement of direct combustion noise in turbopropulsion systems. J. Aircraft 14, (1977) 850–859.
3. P.Y. HO, V.L. Doyle, Combustion noise prediction update. AIAA Paper 79-0588 (1979).
4. E. Krejsa, Highlights of combustion and turbine noise research from the 1970's and 1980's. Proceedings of the Core Noise Workshop sponsored by the Aeroacoustics Research Consortium, February 2003, Phoenix, Arizona.
5. K.K. Singh, S.H. Frankel, J.P. Gore, Effects of combustion on sound pressure generated by circular jet flows. AIAA Journal 41 (2003) 319–321.
6. K.K. Singh, S.H. Frankel, J.P. Gore, Study of spectral noise emissions from standard turbulent nonpremixed flames. AIAA Journal 42 (2004) 931–936.
7. R. Rajaram, T. Lieuwen, Effect of approach flow turbulence characteristics on sound generation from premixed flames, AIAA Paper 2004-0461 (2004).
8. R. Rajaram, T. Lieuwen, Parametric studies of acoustic radiation from premixed flames. Combustion Science and Technology 175 (2003) 2269–2298.
9. J.R. Mahan, A critical review of noise production models for turbulent gas-fueled burners. NASA Report 3803 (1984).
10. S. Kotake, K. Takamoto, Combustion noise: effects of the shape and size of burner nozzle. Journal of Sound and Vibration 112 (1987) 345–354.
11. S. Kotake, K. Takamoto, Combustion noise : Effects of the velocity turbulence of unburned mixture. Journal of Sound and Vibration 139 (1990) 9–20.
12. J. Stephenson , H. Hassan, The spectrum of combustion generated noise, Journal of Sound and Vibration 53 (1977) 283–288.
13. B.N. Shivshankara, W.C. Strahle, J.C. Handley, Combustion noise radiation by open turbulent flames. Progress in Astronautics and Aeronautics 37 (1975) 277–296.
14. A.A. Putnam, Combustion roar of seven industrial burners. Journal Inst. Fuel 49 (1976) 135–138.
15. J. Kilham, N. Kirmani, The effect of turbulence on premixed flame noise. Proceedings of the Combustion Institute 17 (1979) 327–336.

16. G. Petala, R. Petala, Diagnostic possibilities on the basis of premixed flame noise levels, Combustion Flame 52 (1983) 137–147.
17. D.I. Abugov, O.I. Obrezkov, Acoustic noise in turbulent flames. Combust. Explo. Shock 14 (1978) 606–612.
18. A. Billiard, Etude experimentale de l'emission sonore des flames turbulentes, Ph. D. Thesis, Universites d'Aix-Marseille (1997).
19. P. Clavin, E. Siggia, Turbulent premixed flames and sound generation. Combustion Science and Technology 78 (1991) 147–155.
20. P. Clavin, Dynamics of combustion fronts in premixed gases: from flames to detonations. Proc. Comb. Inst. 28 (2000), 569–585.
21. R.G. Huff, Theoretical prediction of the acoustic pressure generated by turbulent-flame front interaction. J. Vibr. Acoustics, Stress, and Reliability in Design 108 (1986) 315–321.
22. C.K.W. Tam, M. Golebiowski, J.M. Seiner, On the two components of turbulent mixing noise from supersonic jets. AIAA Paper 96-1716 (1996).
23. M.D. Dahl, D. Papamoschou, Analytical predictions and measurements of the noise radiated form supersonic coaxial jets. AIAA Journal 38(2000) 585–591
24. C.K.W. Tam, Influence of nozzle geometry on the noise of high-speed jets. AIAA Journal 36 (1998) 1396–1400.
25. C.K.W. Tam, K.B.M.Q. Zaman, Subsonic jet noise from non-axisymmetric and tabbed nozzles. AIAA Journal 32 (2000) 592–599.
26. K. Vishwanathan, Analysis of the two similarity components of turbulent mixing noise. AIAA Journal 38 (2002) 1735–1744.
27. K. Vishwanathan, Aeroacoustics of hot jets. AIAA Paper 2002-2481 (2002).
28. J. Atvars, L.K. Schubert, H.S. Ribner, Refraction of sound from a point source placed in an air jet. Journal of the Acoustical Society of America 37 (1965) 168-170.